Supplementary Information

Titanosilicate zeolite precursors for highly efficient oxidation reactions

Risheng Bai,[a,b] M. Teresa Navarro,[b] Yue Song,[a] Tianjun Zhang,[a] Yongcun Zou,[a] Zhaochi Feng,[c] Peng Zhang,[d] Avelino Corma,*[b] and Jihong Yu*[a,e]

[a] State Key Laboratory of Inorganic Synthesis and Preparative Chemistry, College of Chemistry, Jilin University, Changchun 130012, China

[b] Instituto de Tecnología Química, Universitat Politècnica de València-Consejo Superior de Investigaciones Científicas, Avenida de los Naranjos s/n, 46022 Valencia, España

[c] State Key Laboratory of Catalysis, Dalian Institute of Chemical Physics, Chinese Academy of Sciences, Dalian 116023, China

[d] Department of Chemistry, Dalhousie University, Halifax, Nova Scotia B3H 4R2, Canada

[e] International Center of Future Science, Jilin University, Changchun 130012, China

*Author to whom correspondence should be addressed.
Email: jihong@jlu.edu.cn; acorma@itq.upv.es

Table of Contents

Experimental section 3

Reactant agents 3

Preparation of N,N,N,N',N',N'-hexaethyl-1,4-Benzenedimethanaminium hydroxide 3

Preparation of N,N,N,N',N',N'-hexaethyl-[1,1'-Biphenyl]-4,4'-dimethanaminium hydroxide 3

Preparation of N,N'-dicyclohexyl-N,N,N',N'-tetramethyl-1,4-Benzenedimethanaminium hydroxide 3

Characterizations 3

Catalytic tests 3

Oxidative desulfurization of DBT 4

Epoxidation of cyclohexene 4

Supplementary Figures and Tables 5

Fig. S1. XRD pattern, N_2 adsorption and desorption isotherms, and FT-IR pattern of conventional TS-1 zeolite sample (micro-TS-1) 5

Fig. S2. ^{13}C CP MAS NMR spectra of ATZ-TEA, ATZ-TMAda, ATZ-PhHE, ATZ-DPhHE, and ATZ-PhDC samples 6

Fig. S3. TG curves of the ATZ samples 7

Fig. S4. ^{29}Si MAS NMR spectra of ATZ samples and TS-1 zeolite samples 8

Fig. S5. UV-vis spectrum and UV-Raman spectrum excited at 325 nm of conventional TS-1 zeolite sample (micro-TS-1) 9

Fig. S6. XRD patterns and (b) UV-vis spectra of conventional TS-1 zeolite with different crystallization time 10

Fig. S7. N_2 adsorption-desorption isotherms and pore size distributions of the intermediately crystallized TS-1 zeolite (TS-1-inter) 11

Fig. S8. Time-course variation of DBT conversion and ln(c0/ct) over ATZ-TEA catalyst for the oxidative desulfurization of DBT 12

Fig. S9. Pseudo-first-order rate constants with different concentration of ATZ-TEA catalyst for the oxidation of DBT 13

Fig. S10. Pseudo-first-order rate constants for the oxidation of DBT at different temperatures 14

Fig. S11. Conversion of DBT over ATZ-TEA catalyst at different stirring speed 15

Fig. S12. Conversion of Th and DBT over ATZ-TEA and micro-TS-1 catalysts 16

Fig. S13. UV-vis spectra of ATZ-TEA sample before and after treatment with HNO_3 17

Fig. S14. Catalytic oxidation of DBT with TBHP over ATZ-TEA and HNO_3 treated ATZ-TEA catalysts 18

Fig. S15. Recycle tests in the oxidation of DBT over ATZ-TEA catalyst 19

Fig. S16. UV-vis spectrum and N_2 adsorption-desorption isotherm of the ATZ-TEA catalyst sample after ten cycles in the oxidation of DBT 20

Fig. S17. TEM images of the ATZ-TEA catalyst sample after ten cycles in the oxidation of DBT 21

Fig. S18. XRD patterns of the prepared Ti-Beta and the silylated Ti-Beta 22

Fig. S19. TEM images the prepared nano-sized Ti-Beta catalyst 23

Fig. S20. UV-vis spectra of the prepared Ti-Beta and the silylated Ti-Beta-sil catalysts 24

Fig. S21. UV-vis spectra of the prepared ATZ-TEA and the silylated ATZ-TEA-sil catalysts 25

Table S1. Syntheses and textural porosities of the ZTA samples 26

Table S2. Thermogravimetric (TG) analyses of the as-synthesized ATZ samples 27

Table S3. Structural parameters of ATZ-TEA and TS-1 samples extracted from the EXAFS fitting 28

Table S4. Relative crystallinity of microporous TS-1 zeolite samples at different crystallization time 29

Table S5. Oxidation of cyclohexene over ATZ-TEA 30
Table S6. Oxidation of cyclohexene over TS-1 31
Table S7. Oxidation of cyclohexene over Ti-Beta 32
Table S8. Oxidation of cyclohexene over ATZ-TEA-sil 33
Table S9. Oxidation of cyclohexene over Ti-Beta-sil 34

Experimental section

Reactant agents. All reagents were used as purchased commercially without any further purification. Tetraethylorthosilicate (TEOS, Tianjin Fuchen Chemical Reagent Factory), tetraethylammonium hydroxide (TEAOH) (35%, Alfa), tetrapropylammonium hydroxide (TPAOH) (25wt%, Innochem Co., as verified by ICP, this chemical contains ~3 ppm of Na and free of K), tetrabutyl titanate (TBOT, 98%, Guangfu Fine Chemical Research Institute), tert-butyl hydroperoxide (TBHP, 65%, Sinopharm Chemical Reagent Co.). Nitric acid (69%) and 1-octane were purchased from Beijing Chemical Works. Dibenzothiophene (DBT) (98%), 1,4-bis(bromomethyl)benzene (97%), 4,4'-bis(bromomethyl)biphenyl (97%), N,N-dimethylcyclohexylamine (98%), and trietylyamine (99.5%) were purchased from Energy Chemical Co. Thiophene (99%), tetraethyl orthotitanate (TEOT), dimethoxydimethylsilane (99.5%), triethylamine (99%) tert-butyl hydroperoxide (TBHP, ~5.5 M in decane), and cyclohexene (99%) were purchased from Sigma-Aldrich.

Preparation of N,N,N,N',N',N'-hexaethyl-1,4-Benzenedimethanaminium hydroxide. A total of 27.21 g (100 mmol) of 1,4-bis(bromomethyl)benzene, 22.37 g (220 mmol) of triethylamine and 200 mL ethanol were mixed in a 500 mL flask, and heated under reflux for 96 hours. Then the solution was evaporated to remove all the remaining solvent in a rotavapor. The product was washed with 200 mL ethyl acetate and 200 mL acetone alternatively, and then the white solid obtained was dried under a vacuum providing the desired salt in bromide form. The product is exchanged to the hydroxide form with an anionic exchange Amberlite IRN-78 resin in batch overnight.

Preparation of N,N,N,N',N',N'-hexaethyl-[1,1'-Biphenyl]-4,4'-dimethanaminium hydroxide. A total of 17.00 g (50 mmol) of 4,4'-bis(bromomethyl)biphenyl, 11.13 g (110 mmol) of triethylamine and 100 mL ethanol were mixed in a 250 mL flask, and heated under reflux for 96 hours. Then the solution was evaporated to remove all the remaining solvent in a rotavapor. The product was washed with 100 mL ethyl acetate and 100 mL acetone alternatively, and then the white solid obtained was dried under a vacuum providing the desired salt in bromide form. The product is exchanged to the hydroxide form with an anionic exchange Amberlite IRN-78 resin in batch overnight.

Preparation of N,N'-dicyclohexyl-N,N,N',N'-tetramethyl-1,4-Benzenedimethanaminium hydroxide. A total of 27.21 g (100 mmol) of 1,4-bis(bromomethyl)benzene, 28.56 g (220 mmol) of N,N-dimethylcyclohexylamine and 200 mL ethanol were mixed in a 500 mL flask, and heated under reflux for 96 hours. Then the solution was evaporated to remove all the remaining solvent in a rotavapor. The product was washed with 200 mL ethyl acetate and 200 mL acetone alternatively, and then the white solid obtained was dried under a vacuum providing the desired salt in bromide form. The product is exchanged to the hydroxide form with an anionic exchange Amberlite IRN-78 resin in batch overnight.

Characterizations

Powder X-ray diffraction analysis of the samples was carried out on a Rigaku D-Max 2550 diffractometer using Cu Kα radiation (λ = 1.5418 Å, 50 KV). Transmission electron microscopy (TEM) images were recorded on JEM-2200FS and Tecnai F20 electron microscope. Nitrogen adsorption-desorption measure-ments were carried out on a Micromeritics ASAP 3-flex analyser at 77 K. Before starting the N2 adsorption meas-urements, all the samples were activated by degassing in-situ at about 573 K for 10 h. Chemical compositions were determined with Inductively Coupled Plasma-Optical Emission Spectrometry (ICP-OES) analysis performed on an iCAP 7000 SERIES. The Ultraviolet Visible diffuse reflectance spectroscopy (UV-Vis DRS) of the catalysts was recorded over the range of 190 nm to 500 nm against the support as reference, on a SHIMADZU U-4100. Infrared spectra (IR) were recorded by Nicolet Impact 410 FTIR Infrared Instrument using KBr pellet technique. Ultraviolet Raman resonance spectroscopy (UV-Raman) were recorded on a DL-2 Raman spectrometer using the 266 or 325 nm line of a He-Ge laser as the excitation source and a Princeton CCD as the detector. Thermogravimetric (TG) analysis was performed with a TA company TGA Q500 in air atmosphere with a heating rate of 10 °C/min from room temperature to 800 °C. X-ray absorption spectroscopy data were collected at the Sector 20-BM beamline of the Advanced Photon Source at Argonne National Laboratory. Sample powders were packed on plastic washer and folded multiple times to enhance the signal. The beamline was equipped with a doublecrystal Si (111) monochromator. A 12-element Ge fluorescence detector was used to collect spectra of the Ti K-edge. Data processing and EXAFS fitting

were performed using the Athena, Artemis and Igor software.

Catalytic tests

Oxidative desulfurization of thiophene (Th) and dibenzothiophene (DBT).

Th or DBT was dissolved in n-octane to prepare the model fuel with sulfur concentration of about 500 ppm. The oxidative desulfurization reaction was performed in a 50 mL three-necked round-bottom flask, connected to a reflux cooler system with magnetic stirring. The catalyst was activated at 200 °C for 2h before used. Typically, 20 mg catalyst was added into 10 mL of model fuel, then n-octadecane and proper amount of TBHP were added in turn, which acted as internal standard and oxidant, respectively. The reaction was carried at 333K for 15 min under magnetic stirring of 600 rpm to eliminate the effects of the external mass transfer resistances of the catalysts. The conversion of TBHP was determined by the titration of $Ce(SO_4)_2$ with Ferroin as an indicator. The products were analyzed by Gas Chromatography-Mass Spectrometry (GC-MS, Thermo Fisher Trace ISQ, equipped with TG-5MS column, L=60 m). Mass balances were accurate to within 5%.

Epoxidation of cyclohexene.

The epoxidation of cyclohexene with TBHP as oxidant and undecane as internal standard was carried out in batch reactors. The catalyst was activated at 200 °C for 2h before used. In a typical run, cyclohexene (56 mmol), TBHP 5.5M in decane (14 mmol), and catalyst (30 mg) were added into the batch reactor and pressurized the reactor to 3 bars of nitrogen. The reaction was carried at 333 K. Sample analyses were performed on a GC-system with FID detector and a polar column (HP-5, L=30m). Mass balances were accurate to within 5%.

Supplementary Figures and Tables

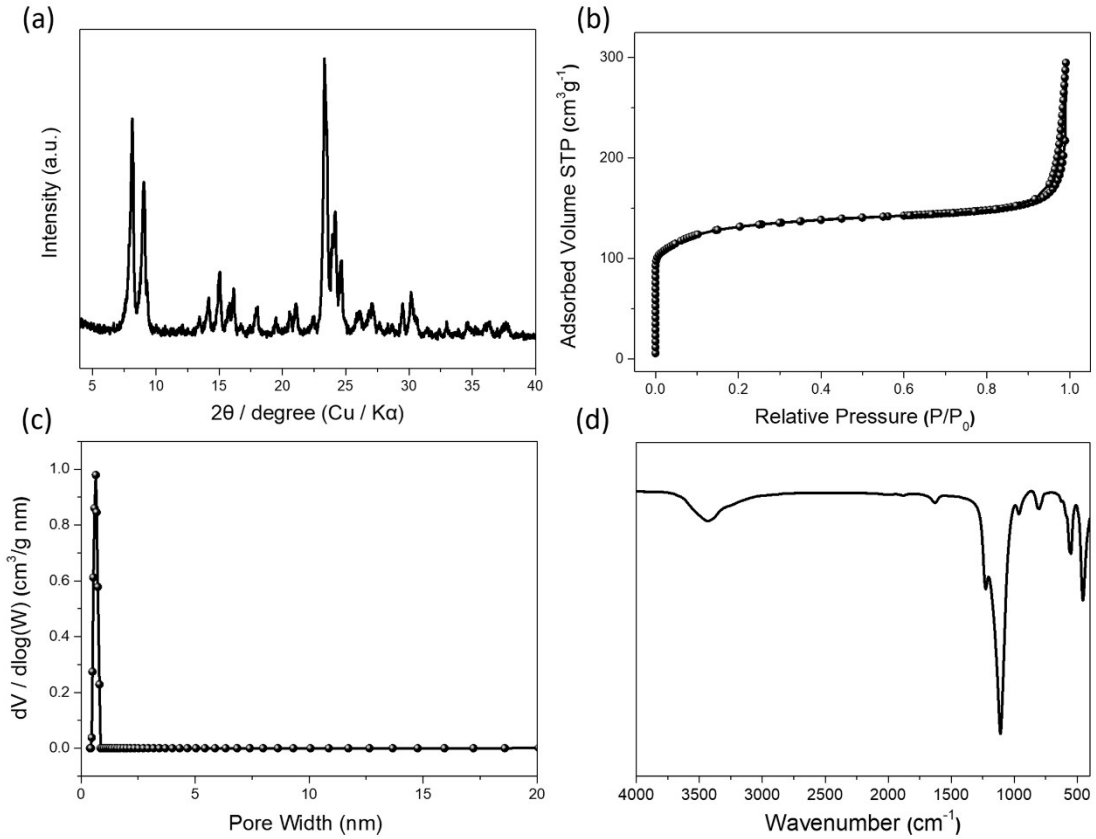

Fig. S1. (a) XRD pattern, (b) N_2 adsorption and desorption isotherms, (c) pore size distribution, and (d) FT-IR pattern of conventional TS-1 zeolite sample (micro-TS-1).

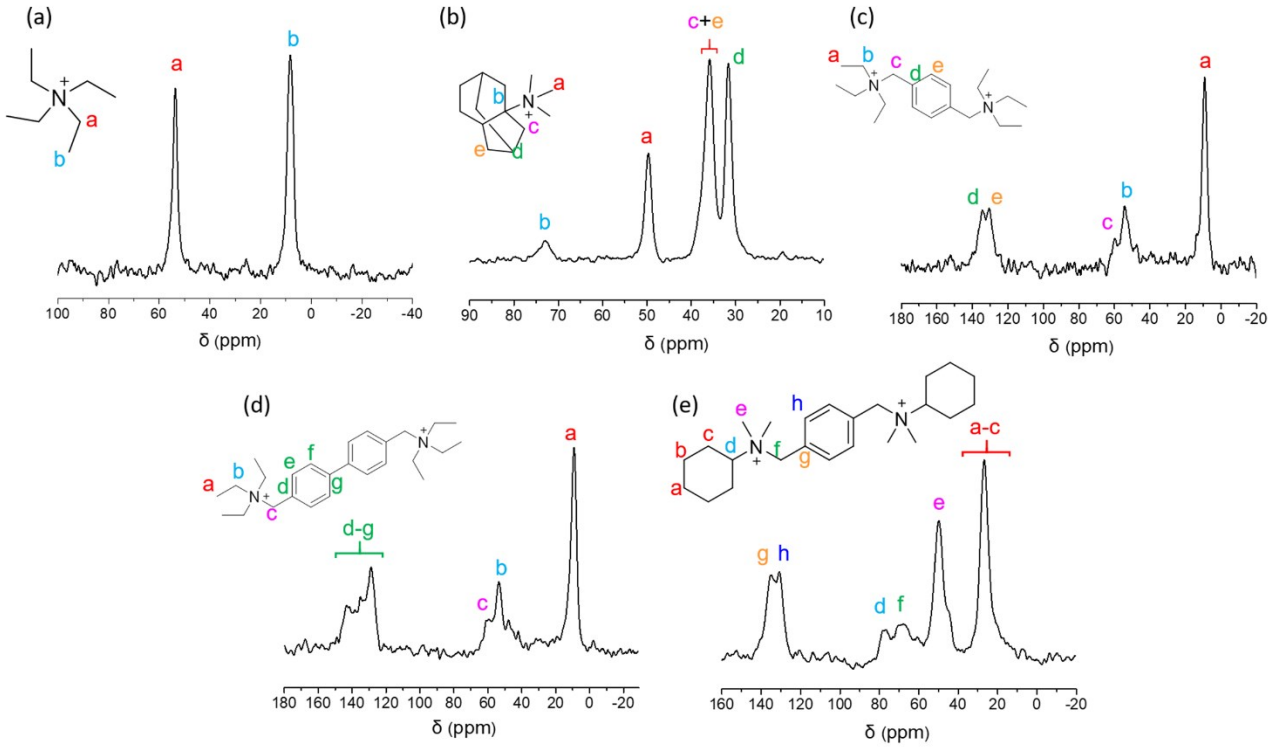

Fig. S2. ^{13}C CP MAS NMR spectra of (a) ATZ-TEA, (b) ATZ-TMAda, (c) ATZ-PhHE, (d) ATZ-DPhHE, and (e) ATZ-PhDC samples.

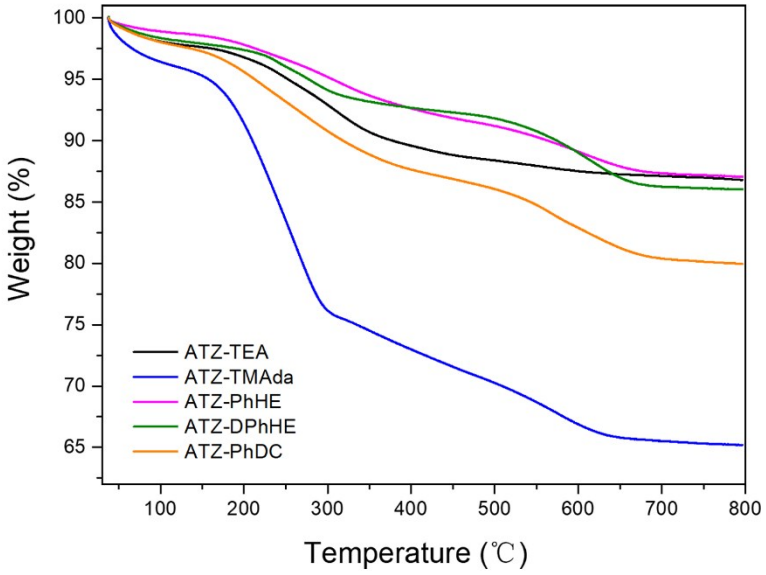

Fig. S3. TG curves of the ATZ samples.

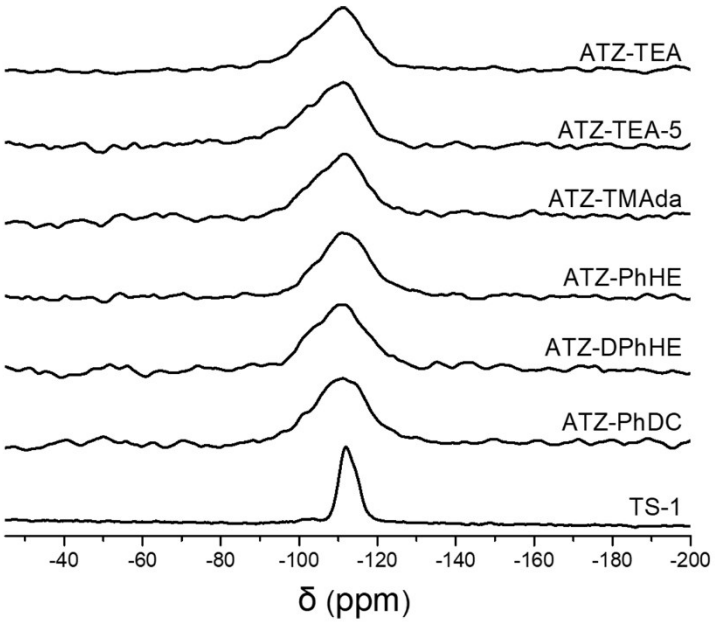

Fig. S4. ^{29}Si MAS NMR spectra of ATZ samples and TS-1 zeolite samples.

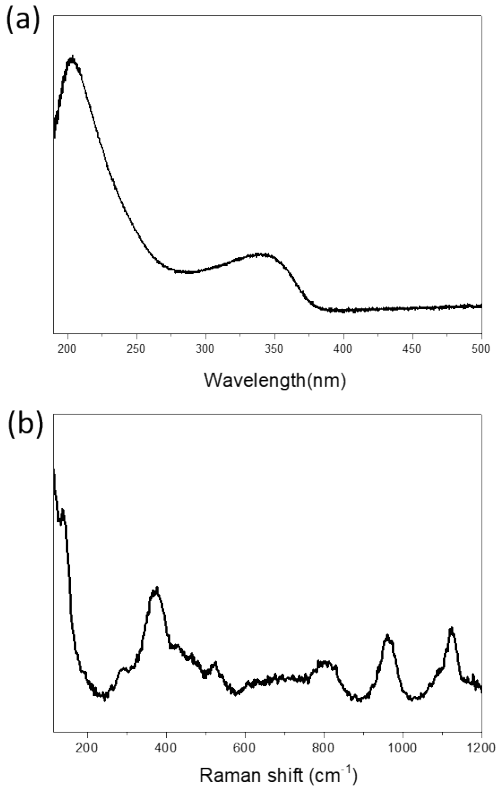

Fig. S5. (a) UV-vis spectrum and (b) UV-Raman spectrum excited at 325 nm of conventional TS-1 zeolite sample (micro-TS-1).

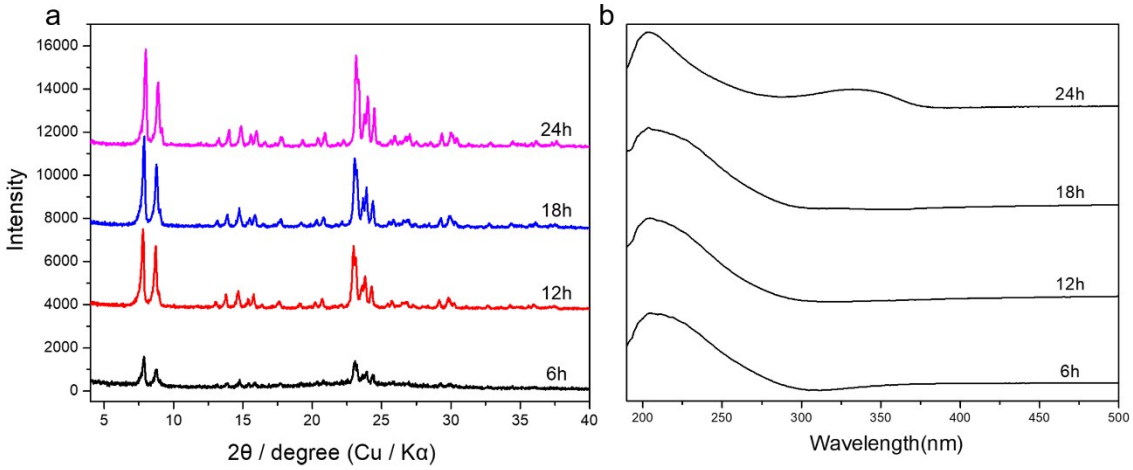

Fig. S6. (a) XRD patterns and (b) UV-vis spectra of conventional TS-1 zeolite with different crystallization time.

It can be seen that with the crystallization process prolonged, the relative crystallinity increased while the amount of octahedrally coordinated Ti decreased, and the anatase species appeared.

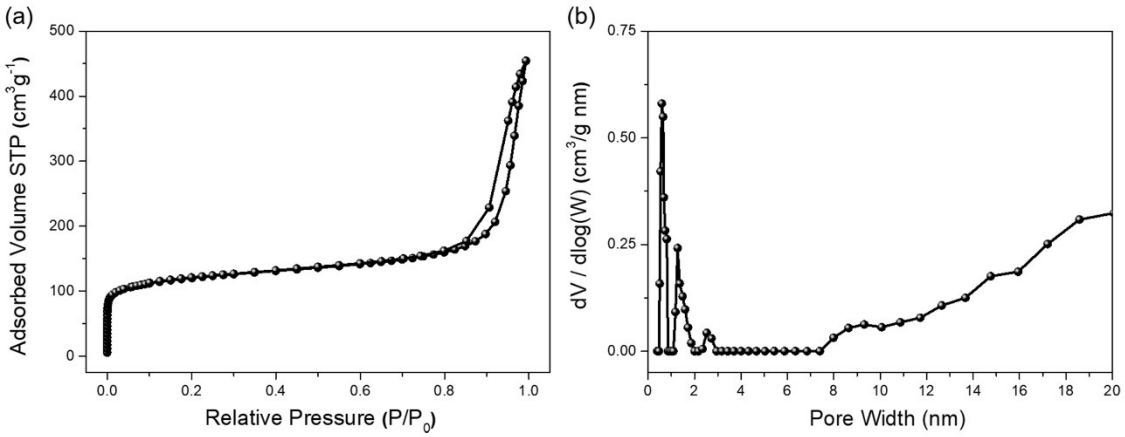

Fig. S7. (a) N_2 adsorption-desorption isotherms and (b) pore size distributions of the intermediately crystallized TS-1 zeolite (TS-1-inter).

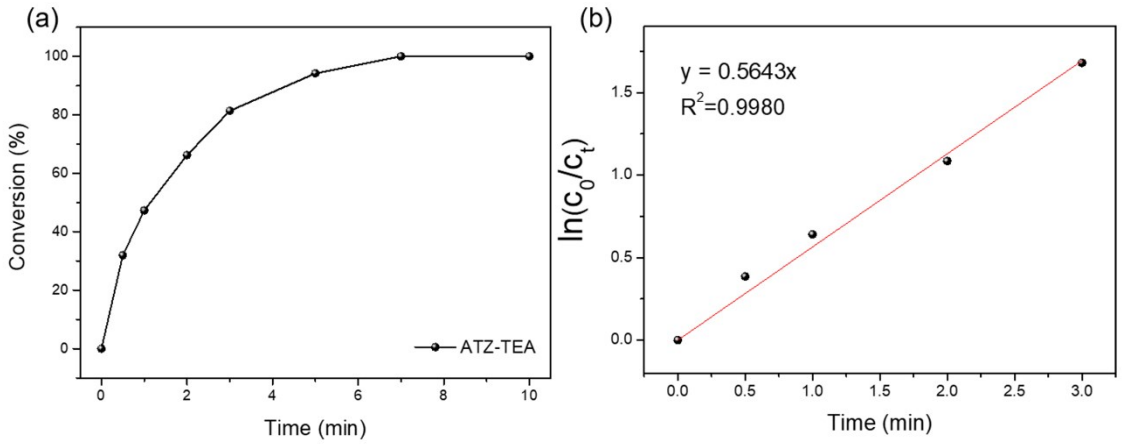

Fig. S8. (a) Time-course variation of DBT conversion and (b) ln(c0/ct) over ATZ-TEA catalyst. Reaction conditions: 10mL of 500 ppm model fuels, 20mg of ATZ-TEA catalyst, n(sulphide)/n(TBHP) was 0.5, 333K, 10 min.

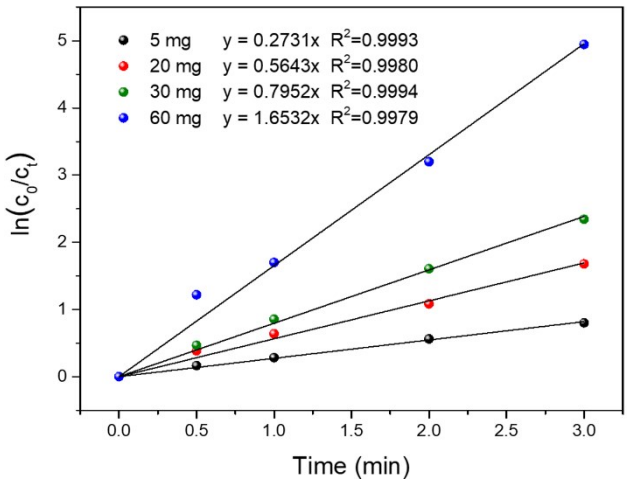

Fig. S9. Pseudo-first-order rate constants with different concentration of ATZ-TEA catalyst for the oxidation of DBT. Reaction conditions: 10mL of 500 ppm model fuel, n(sulphide)/n(TBHP) was 0.5, 333K.

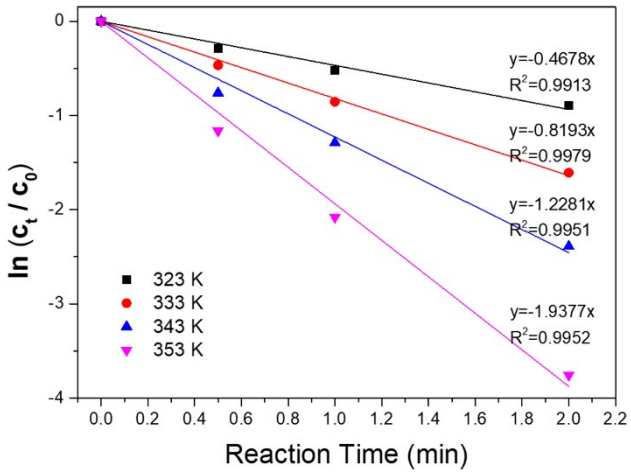

Fig. S10. Pseudo-first-order rate constants for the oxidation of DBT at different temperatures. Reaction conditions: 10mL of 500 ppm model fuel, 30mg of ATZ-TEA catalyst, n(sulphide)/n(TBHP) was 0.5.

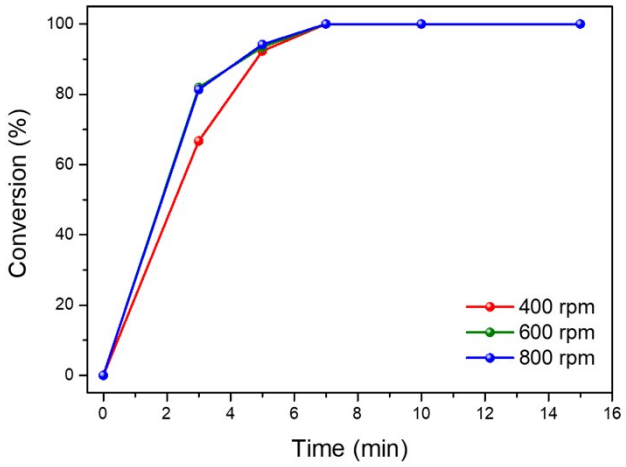

Fig. S11. Conversion of DBT over ATZ-TEA catalyst at different stirring speed. Reaction conditions: 10mL of 500 ppm model fuels, 20mg of ATZ-TEA catalyst, n(sulphide)/n(TBHP) was 0.5, 333K, 15 min.

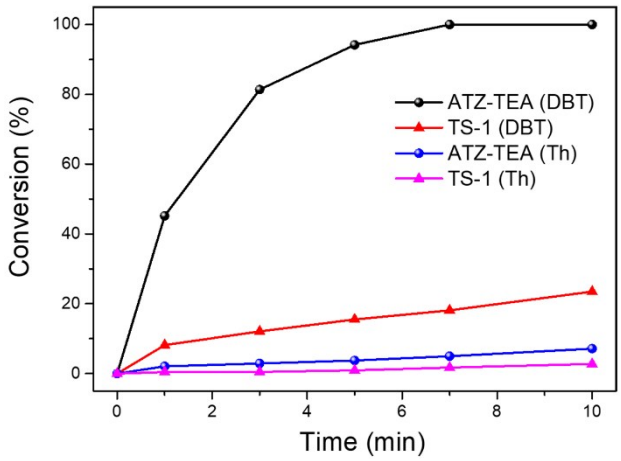

Fig. S12. Conversion of Thiophene (Th) and DBT over ATZ-TEA and micro-TS-1 catalysts. Reaction conditions: 10mL of 500 ppm model fuels, 20mg of catalyst, n(sulphide)/n(TBHP) was 0.5, 333K, 10 min.

Note: We measured the rate of the reaction for two reactants with different molecular size: thiophene (Th) and dibenzothiophene (DBT). Thiophene could penetrate, at least some, within TS-1, while dibenzothiophene cannot penetrate within the pores of MFI. Then we have measured the initial rate for the oxidative desulfurization of the two molecules with the microporous TS-1 and the amorphous titanosilicate zeolite precursor (ATZ-TEA) that contains extra-large pores. The results show that with the larger dibenzothiophene molecule, the ratio of the initial reaction rate, with respect to thiophene, is much larger with the amorphous titanosilicate zeolite precursor with extra-large pores than with TS-1.

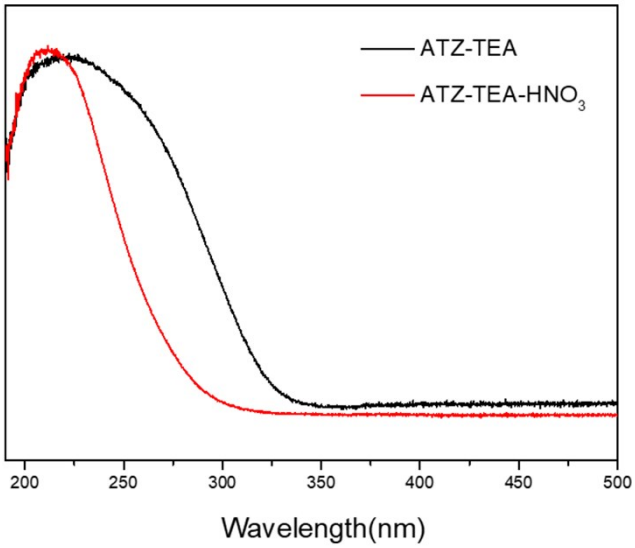

Fig. S13. UV-vis spectra of ATZ-TEA sample before and after treatment with HNO_3.

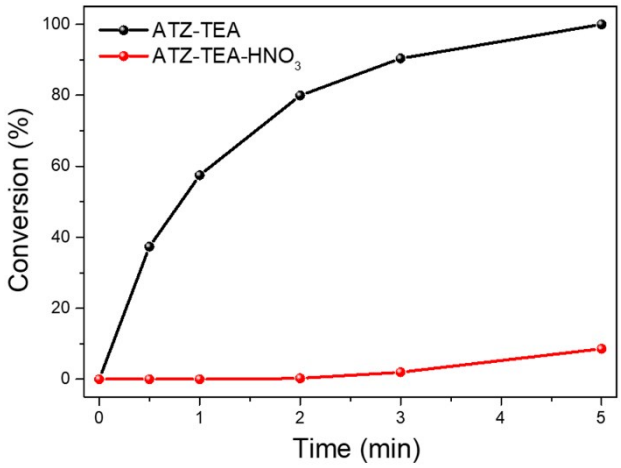

Fig. S14. Catalytic oxidation of DBT with TBHP over ATZ-TEA and HNO_3 treated ATZ-TEA catalysts.

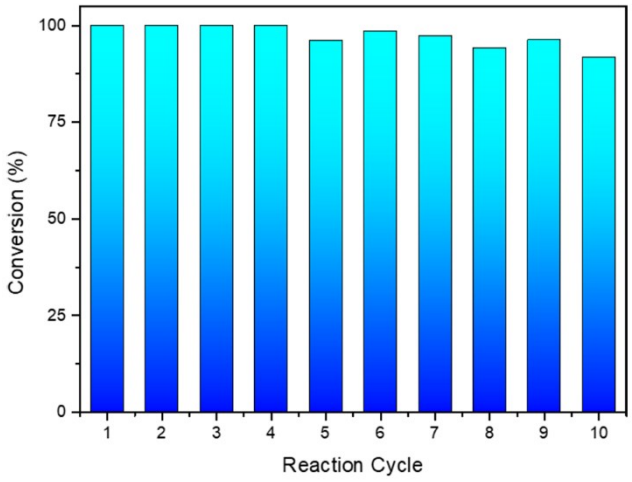

Fig. S15. Recycle tests in the oxidation of DBT over ATZ-TEA catalyst. Reaction condition: 10 mL 500 ppm DBT model fuels, 30mg of ATZ-TEA catalyst, n(sulphide)/n(TBHP) was 0.5, 333K, 10 min.

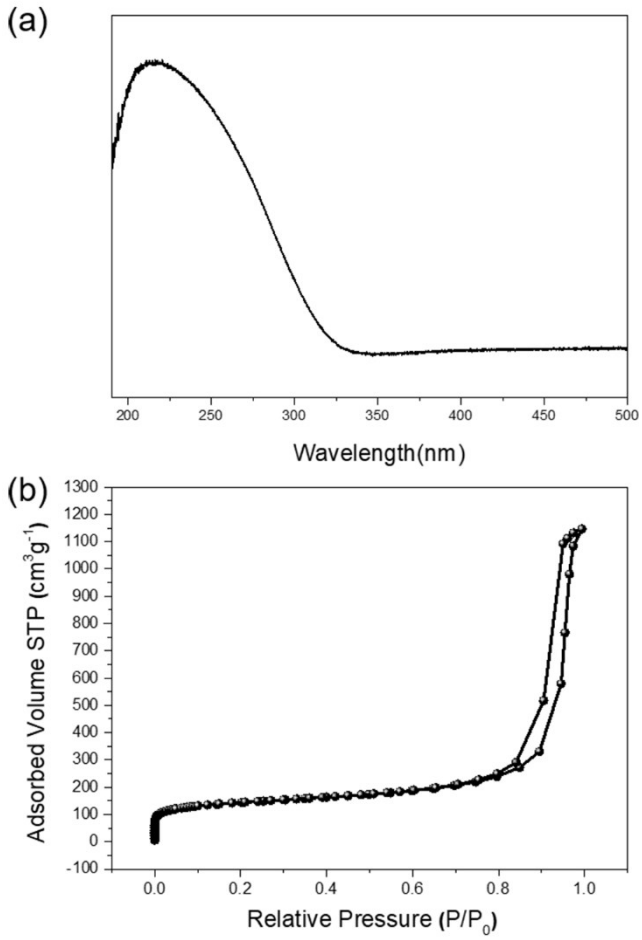

Fig. S16. (a) UV-vis spectrum and (b) N_2 adsorption-desorption isotherm of the ATZ-TEA catalyst sample after ten cycles in the oxidation of DBT.

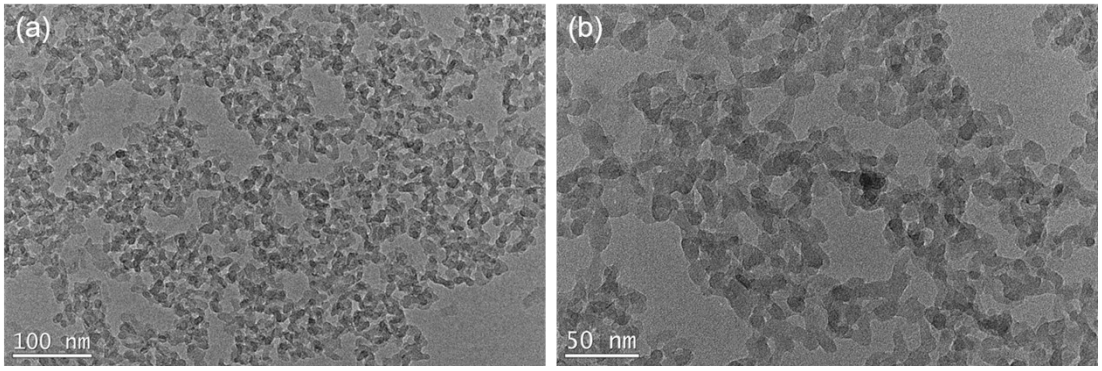

Fig. S17. TEM images of the ATZ-TEA catalyst sample after ten cycles in the oxidation of DBT.

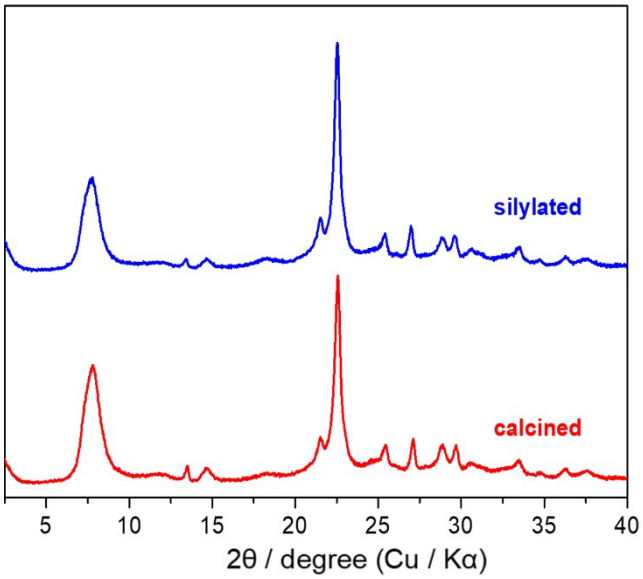

Fig. S18. XRD patterns of the prepared Ti-Beta and the silylated Ti-Beta.

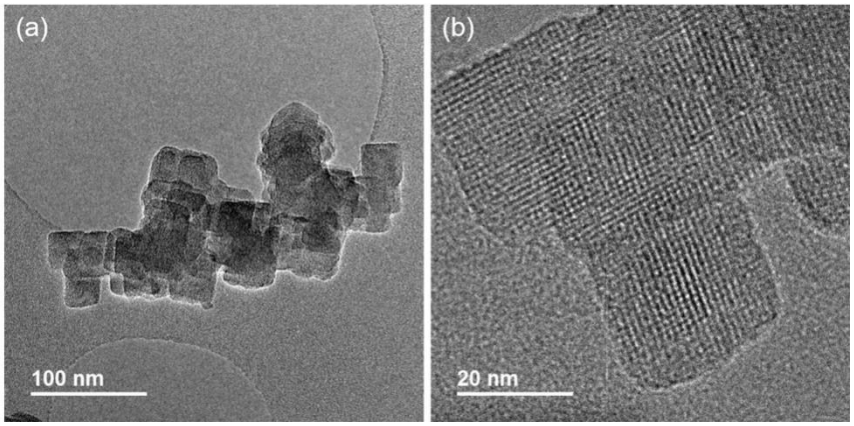

Fig. S19. TEM images the prepared nano-sized Ti-Beta catalyst.

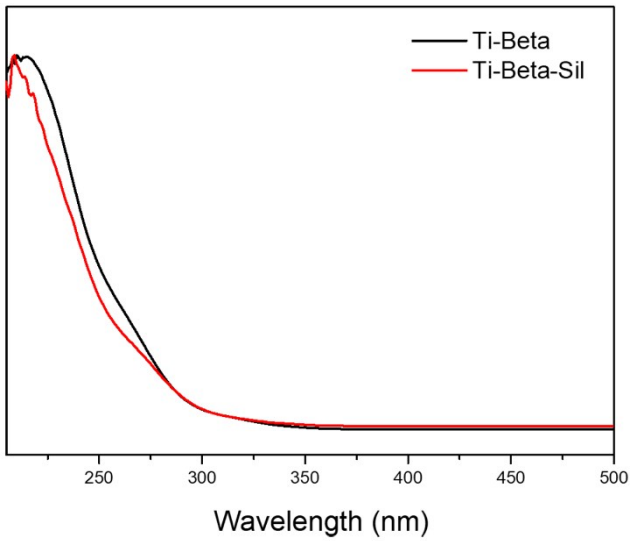

Fig. S20. UV-vis spectra of the prepared Ti-Beta and the silylated Ti-Beta-sil catalysts.

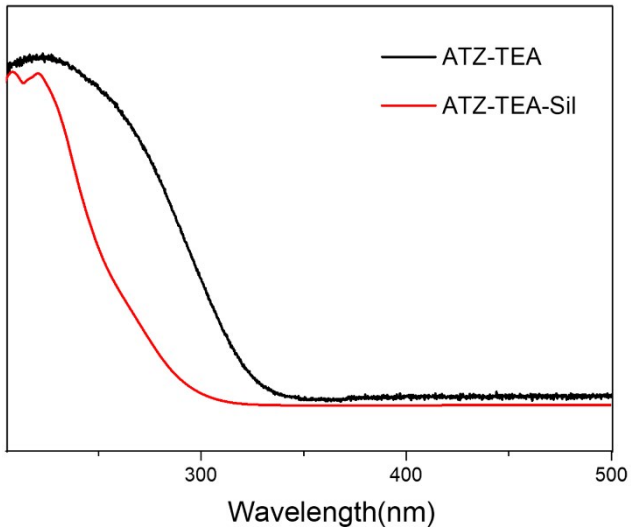

Fig. S21. UV-vis spectra of the prepared ATZ-TEA and the silylated ATZ-TEA-sil catalysts.

Table S1. Syntheses and textural porosities of the ATZ samples.

Sample	Si/Ti[b]	S_{BET}[c] (m^2/g)	S_{micro}[c] (m^2/g)	S_{ext}[c] (m^2/g)	V_{total}[d] (cm^3/g)	V_{micro}[c] (cm^3/g)	V_{meso}[e] (cm^3/g)	$I_{960/800}$[f]
ATZ-TEA[a]	58.0	524	275	249	1.78	0.11	1.67	-
TS-1-inter (6h)	86.6	373	187	186	0.70	0.10	0.60	-
micro-TS-1 (24h)	43.2	495	343	152	0.43	0.13	0.30	1.16

[a]The catalyst was used after 10 reaction-regeneration cycle times. [b]Measured by inductively coupled plasma (ICP). [c]Specific surface area calculated from the nitrogen adsorption isotherm using the BET method. [c]S_{micro} (micropore area), S_{ext} (external surface area), and V_{micro} (micropore volume) calculated using the t-plot method. [d]Total pore volume at $P/P_0 = 0.995$. [e]$V_{meso} = V_{total} - V_{micro}$. [f]FT-IR relative intensity of the bands at 960 and 800 cm^{-1}

Table S2. Thermogravimetric (TG) analyses of the as-synthesized ATZ samples.

		H_2O weight loss (%)	Template weight loss (%)	Template weight loss (%)	Total (%)
ATZ-TEA	Temperature (°C)	35-170	170-350	350-800	13.1
	Weight loss (%)	2.6	6.8	3.7	
ATZ-TMAda	Temperature (°C)	35-150	150-300	300-800	34.8
	Weight loss (%)	4.6	19.4	10.8	
ATZ-PhHE	Temperature (°C)	35-180	180-350	350-800	13.0
	Weight loss (%)	1.7	4.8	6.5	
ATZ-DPhHE	Temperature (°C)	35-220	220-350	350-800	14.0
	Weight loss (%)	3.0	3.9	7.1	
ATZ-PhDC	Temperature (°C)	35-150	150-400	400-800	20.0
	Weight loss (%)	2.8	9.6	7.6	

Table S3. Structural parameters of ATZ-TEA and TS-1 samples extracted from the EXAFS fitting.

Sample	Shell	Coordination Number	σ^2(Å^2)[a]	R (Å)[b]	ΔE_0 (eV)[c]	R-factor (%)[d]
ATZ-TEA	Ti-O	3.6 +/- 0.5	0.0022 +/- 0.0015	1.84 +/- 0.01	7.4 +/- 2.5	0.008
TS-1-TiO4	Ti-O	4.0	0.0004 +/- 0.0019	1.82 +/- 0.02	6.8 +/- 2.4	0.022

[a] σ^2 is Debye-Waller factor (a measure of thermal and static disorder in absorber-scatterer distances); [b] R is bond distance; [c] ΔE_0 is edge energy shift (the difference between the zero-kinetic energy value of the sample and that of the theoretical model). [d] R factor is used to value the goodness of the fitting.

Table S4. Relative crystallinity of microporous TS-1 zeolite samples at different crystallization time.

	Intensity of Peaks[a]			Relative
	23.1°	24.0°	24.5°	Crystallinity (%)[b]
TS-1-6h (TS-1-inter)	1390	900	730	39.6
TS-1-12h	2455	1570	1095	67.1
TS-1-18h	3280	1940	1305	85.5
TS-1-24h (micro-TS-1)	3380	2400	1855	100.0

[a]Based on the XRD patterns of samples in Figure R5a. [b]The relative crystallinity is calculated based on the intensity of the three peaks (2θ=23.1°, 24.0°, and 24.5°) in the XRD patterns in Fig. S6a.

Table S5. Oxidation of cyclohexene over ATZ-TEA.[a]

Reaction Time (h)	Conv.		TBHP		Select. (%)					
	(%)	max (%)	Conv. (%)	Effic. (%)	Epoxide	Cyc6=_ol	Cyc6=one	Glycol	dimer	ether
1	6.0	24.0	26.2	93.5	49.6	25.2	9.3	16.0	0	0
2	7.9	31.4	35.1	91.3	61.1	23.4	6.5	9.0	0	0
3	8.8	35.2	38.6	93.0	64.7	23.1	6.2	6.0	0	0
5	10.4	41.6	44.8	94.8	69.3	21.4	3.6	5.7	0	0

[a]Reaction conditions: cat., 30 mg; cyclohexene, 56 mmol; TBHP (80 wt%), 14 mmol; temp., 333 K, 3 bar of N_2.

Table S6. Oxidation of cyclohexene over TS-1.[a]

Reaction Time (h)	Conv.		TBHP		Select. (%)					
	(%)	max (%)	Conv. (%)	Effic. (%)	Epoxide	Cyc6=_ol	Cyc6=one	Glycol	dimer	ether
1	3.7	14.9	17.1	88.9	10.9	23.0	17.6	48.6	0	0
2	3.8	15.3	18.0	86.8	11.3	23.7	18.2	46.8	0	0
3	3.9	15.7	18.3	87.5	11.1	23.4	17.4	48.2	0	0
5	4.0	15.8	18.8	86.1	11.4	24.0	17.9	46.8	0	0

[a]Reaction conditions: cat., 30 mg; cyclohexene, 56 mmol; TBHP (80 wt%), 14 mmol; temp., 333 K, 3 bar of N_2.

Table S7. Oxidation of cyclohexene over Ti-Beta.[a]

Reaction Time (h)	Conv.		TBHP		Select. (%)					
	(%)	max (%)	Conv. (%)	Effic. (%)	Epoxide	Cyc6=_ol	Cyc6=one	Glycol	dimer	ether
1	5.2	20.9	25.1	85.0	38.6	22.6	11.8	27.0	0	0
2	5.7	22.6	25.3	91.2	43.3	22.5	11.5	22.7	0	0
3	6.5	26.0	27.1	98.3	43.2	21.7	9.6	25.6	0	0
5	6.9	27.6	30.5	92.3	43.8	23.1	9.7	23.5	0	0

[a]Reaction conditions: cat., 30 mg; cyclohexene, 56 mmol; TBHP (80 wt%), 14 mmol; temp., 333 K, 3 bar of N_2.

Table S8. Oxidation of cyclohexene over ATZ-TEA-sil.[a]

Reaction Time (h)	Conv.		TBHP		Select. (%)					
	(%)	max (%)	Conv. (%)	Effic. (%)	Epoxide	Cyc6=_ol	Cyc6=one	Glycol	dimer	ether
1	10.8	43.0	44.7	98.3	78.4	17.9	2.6	1.1	0	0
2	14.1	56.2	57.7	99.4	82.3	15.0	1.7	1.1	0	0
3	15.6	62.3	64.1	99.3	84.3	13.4	1.3	1.0	0	0
5	17.7	70.7	72.8	99.1	86.1	11.7	1.6	1.1	0	0

[a]Reaction conditions: cat., 30 mg; cyclohexene, 56 mmol; TBHP (80 wt%), 14 mmol; temp., 333 K, 3 bar of N_2.

Table S9. Oxidation of cyclohexene over Ti-Beta-sil.[a]

Reaction Time (h)	Conv.		TBHP		Select. (%)					
	(%)	max (%)	Conv. (%)	Effic. (%)	Epoxide	Cyc6=_ol	Cyc6=one	Glycol	dimer	ether
1	5.5	22.3	24.8	80.9	23.7	25.9	13.3	28.9	0	0
2	6.0	24.5	22.9	96.3	31.9	24.8	15.8	35.7	0	0
3	6.1	25.1	25.6	88.0	36.7	25.7	11.4	26.2	0	0
5	7.3	29.8	27.7	96.8	46.5	27.5	9.3	16.8	0	0

[a]Reaction conditions: cat., 30 mg; cyclohexene, 56 mmol; TBHP (80 wt%), 14 mmol; temp., 333 K, 3 bar of N_2.